Advances in Nano Research, *Vol. 9, No. 3 (2020) 173-181*
DOI: https://doi.org/10.12989/anr.2020.9.3.173

Adsorption and electro-Fenton processes over FeZSM-5 nano-zeolite for tetracycline removal from wastewater

Hadi Adel Niaei[1,2] and Mohammad Rostamizadeh*[1,2]

[1]*Faculty of Chemical Engineering, Sahand University of Technology, Sahand New Town, Tabriz, Iran, P.O. Box: 51335-1996*
[2]*Research Center of Environmental Engineering, Sahand University of Technology, Sahand New Town, Tabriz, Iran, P.O. Box: 51335-1996*

(*Received April 13, 2019, Revised August 23, 2020, Accepted October 8, 2020*)

Abstract. Adsorption and heterogeneous electro-Fenton process using iron-loaded ZSM-5 nano-zeolite were investigated for the removal of Tetracycline (TC) from wastewater. The nano-zeolite was synthesized hydrothermally and modified through impregnation. The zeolite was characterized by XRD, FT-IR, FE-SEM, N_2 adsorption-desorption, and NH_3-TPD techniques. The equilibrium data were best represented by the Freundlich isotherm. The pseudo-second-order kinetic model was the most accurate model for the adsorption of TC on the modified nano-zeolite. The effect of parameters such as pH of solution and current density were investigated for the heterogeneous electro–Fenton process. The results showed that the current density of 150 mA and pH of 3 led to the highest TC removal (90.35%) at 50 min. The nano-zeolite showed the appropriate reusability. Furthermore, the developed kinetic model was in good agreement with the removal data of TC through the electro-Fenton process.

Keywords: adsorption; electro-Fenton; kinetic; nano-zeolite; pharmaceutical

1. Introduction

Tetracycline (TC) was discovered in the 1940s, which is an important antibiotic for prophylaxis and treatment of infectious diseases. In the United States, TC are added at sub therapeutic levels to animal feeds to act as growth promoter (Chopra and Roberts 2001, Eliopoulos *et al*. 2003). Therefore, large amount of contamination from this drug can be released into the environment. Biological methods are difficult to achieve complete removal of TC (Ali *et al*. 2009). So, chemical and physical methods have attracted much attention. Adsorption and Advanced Oxidation Processes (AOPs) are the most effective techniques for the removal of various organic pollutants due to the low cost, simple operation and easy maintenance (Álvarez-Torrellas *et al*. 2016, Vosoughi *et al*. 2017). AOPs are based on the production of hydroxyl radicals (˙OH), as a strong oxidant agent, for the mineralization of organic compounds to CO_2 and H_2O. ˙OH can be produced by different methods such as Fenton process, photochemistry (photo-Fenton, heterogeneous photo catalysis) and electro chemistry (Gharibian *et al*. 2020, Martínez-Huitle and Brillas 2008). The electro-Fenton is the combination of two processes of anodic oxidation and Fenton (Brillas *et al*. 2009, Panizza and Cerisola 2009). In this method, chemical generation of ˙OH is carried out by the classical Fenton's reaction (Eq. (1)) through a mixture of the electrical synthesis of H_2O_2 (Eq. (2)) and a soluble Ferrous iron (Fe^{2+}). At the next step, formed Ferric iron (Fe^{3+}) at the cathode reduces to Fe^{2+} (Eq. (3)).

$$H_2O_2 + Fe^{2+} \rightarrow Fe^{3+} + OH^- + {}^{\cdot}OH \quad (1)$$

$$O_2 + 2H^+ + 2e^- \rightarrow H_2O_2 \quad (2)$$

$$Fe^{3+} + e^- \rightarrow Fe^{2+} \quad (3)$$

Zeolites are crystalline aluminosilicates with high porosity where AlO_4 and SiO_4 are connected by oxygen atoms. The presence of AlO_4 in zeolite induces a negative charge in the structure of these materials that is neutralized by the presence of cations such as Na, K, Ca and Mg. Zeolites are used in the industry as adsorbents, ion exchangers, and molecular sieves. One of the common zeolites is ZSM-5 (Chu *et al*. 2017, Rostamizadeh and Rizi 2012). Due to the high specification properties, stability, and the porous structure, it can be applied as an adsorbent and catalyst to organic pollutant removal from water. Basu and Barman (2019) studied the adsorption of fipronil from aqueous solution by modified zeolite HZSM-5. The zeolite was modified with 5%, 10%, 15%, 20%, 25% and 30% wt% of cerium nitrate solution. The maximum adsorption capacity was found for Ce_{22}ZSM-5 sample (598.8 mg g^{-1}) in 120 min. Furthermore, several investigations have been conducted on TC removal from water using various adsorbents. Ifebajo *et al*. (2019) studied the adsorption of TC using $CoO/CuFe_2O_4$. The results showed that the TC removal efficiency reached 96.6% at pH = 6. Huang *et al*. (2014) investigated adsorption of TC and ciprofloxacin over activated carbon. They found that the adsorption kinetic well fitted the pseudo-second-order model ($R^2 > 0.99$).

*Corresponding author, Professor,
E-mail: Rostamizadeh.m@gmail.com

ISSN: 2287-237X (Print), 2287-2388 (Online)

Table 1 General information of TC

Name	Chemical structure	Molecular formula	Mw (g mol^{-1})	λ_{max} (nm)
Tetracycline	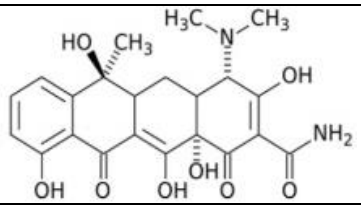	$C_{22}H_{24}N_2O_8$	444.44	358

Ghadim *et al*. (2013) studied the adsorption of TC on graphene oxide. The results showed that the maximum adsorption was 323 mg g^{-1} at 298 K.

On the other hand, different research reported the potential of AOPs for removal of pharmaceutical pollutants from water. Rostamizadeh *et al*. (2019) reported the diclofenac removal using the heterogeneous Fe-ZSM-5 catalyst in the Fenton process at reaction conditions of pH = 3, T = 25°C, $[H_2O_2]$ = 10 ppm and M = 2 gL^{-1}, which led to the removal of 95% diclofenac. Yahya *et al*. (2014) studied the degradation of ciprofloxacin by electro-Fenton process. The results showed 94% efficiency at 400 mA, 0.1 mM Fe^{2+}, and 6 h. Xue *et al*. (2015) compared the efficiency of different AOP methods for the degradation of TC using $BiFeO_3$. The residual TC concentration of the photocatalysis, Fenton, and photo-Fenton processes were 81%, 65% and 21%, respectively. Puga *et al*. (2020) investigated the adsorption/electro-Fenton process of antibiotic removal over iron-doped perlit catalyst. They found that the adsorption process followed the Langmuir isotherm model and the experimental results confirmed the high catalyst activity and antibiotic removal (> 95%). As the best of our knowledge, there is no report for TC removal using iron modified ZSM-5 zeolite through the adsorption/ electro-Fenton process. Therefore, the objective of this work was to investigation of the FeZSM-5 nano-zeolite as an adsorbent/catalyst in the hybrid process of adsorption/ electro-Fenton for TC removal.

2. Materials and methods

2.1 Materials

The reagents were tetra propyl ammonium bromide (TPABr, $C_{12}H_{28}BrN$ > 99 wt%), iron nitrate ($Fe(NO_3)_2$ $.9H_2O$, 99 wt%), silicic acid (SiO_2 $.xH_2O$ > 99% wt), sodium aluminate ($NaAl_2$, Al_2O_3 wt% = 55), ammonium nitrate (NH_4NO_3, 99 wt%), sodium hydroxide (NaOH, 99.6 wt%), and sulfuric acid (H_2SO_4, 98 wt%), which were purchased from Merck company (Germany). The general characterization of TC is presented in Table 1.

2.2 Catalyst preparation

In this study, FeZSM-5 nano-zeolite was prepared by hydrothermal method according to the reported procedure (Rostamizadeh *et al*. 2018b). In this method, silicic acid, sodium hydroxide, TPABr, sodium aluminate, and deionized water were used to synthesis of the parent nano-zeolite ($\frac{Si}{Al} = 200$). The synthesis solution was stirred for 3 h with the mechanical stirrer and appropriate amount of sulfuric acid adjusted the pH (10.5). The molar composition of the synthesis solution was 20 SiO_2 : 0.05 Al_2O_3 : 3 TPABr : 1.5 Na_2O : 200 H_2O. The crystallization of nano-zeolite was applied at 180°C for 48 h under autogenous pressure in a static stainless-steel Teflon-lined autoclave. After filtration and washing, the nano-zeolite was dried at 105°C overnight. Then, the calcination was carried out at 530°C, for 12 h (heating rate of 3°C min^{-1}) in a muffle furnace under air flow. The parent nano-zeolite was denoted by HZSM.

2.3 Impregnation

The impregnation of HZSM-5 nano-zeolite with iron promoter was in rotator evaporator device, including the following five steps:

i. 65°C and 300 mmHg for 60 min
ii. 70°C and 250 mmHg for 30 min
iii. 70°C and 200 mmHg for 30 min
iv. 75°C and 200 mmHg for 30 min
v. 70°C and 180 mmHg for 30 min

After impregnation, the nano-zeolite was dried overnight at 105°C and followed by calcination at 530°C (heating rate of 3°C min^{-1}) for 12 h. The modified nano-zeolite included 0.5 wt% promoter, which was denoted by FeZSM.

2.4 Nano-zeolite characterization

The prepared FeZSM nano-zeolite was characterized by XRD, FT-IR, FE-SEM, N_2 adsorption-desorption and NH_3-TPD. Powder X-ray Diffraction pattern (XRD) of the nano-zeolites was recorded in the range of 2θ = 0-50° with a D8 Advance Bruker AXS X- ray diffractometer, including Ni-filtered Cu Kα radiation (λ = 0.15418 nm). To determine the surface morphology, FE-SEM images were obtained by a KYKY equipment (Model, EM3200). N_2 adsorption-desorption at 77 K was measured using (Quanta chrome, USA) equipment. The FT-IR measurements were recorded in the 400-4000 cm^{-1}, with a Nexus model infrared spectrophotometer (Nicolet Co, USA). Temperature programmed desorption of ammonia (NH_3-TPD) was applied with an on-line TCD detector (Micromeritics, USA), which analyzed acidity the nano-zeolite. Spectrophotometric measurements were conducted using

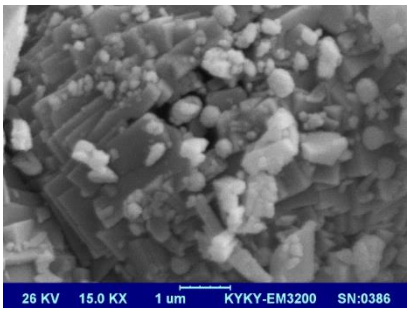

(a)

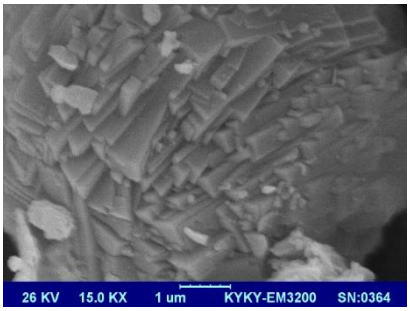

(b)

Fig. 1 FE-SEM image of the nano-zeolite (a) HZSM and (b) FeZSM

Jenway 6705 UV-vis spectrophotometer (England).

2.5 Adsorption isotherm

Adsorption isotherm of TC on FeZSM nano-zeolite was obtained in pH = 3 and 0.3 gL^{-1} of nano-zeolite. The initial concentration of TC solution was 5, 10, 15, 20 and 25 mg L^{-1}. The solution was stirred (160 rpm) for 50 min at 25°C. The data was modeled by Langmuir and Freundlich isotherms.

2.6 Adsorption kinetic

Batch experiments for the adsorption kinetic were performed using 0.3 gL^{-1} of FeZSM and 0.1 L of TC solution in pH = 3. The initial concentration was 10 mg L^{-1} of TC. The solution was stirred (160 rpm) at 25°C for different times (10, 20, 30, 40 and 50 min). After each time, the mixture was then centrifuged at 4000 rpm for 15 min and absorbance of the each sample of the TC solution was analyzed by spectrophotometer at the maximum adsorption wavelength (λ_{max} = 358 nm). The amount of adsorption capacity equilibrium was calculated using Eq. (4).

$$q_e = \frac{C_0 - C_e}{M} \times V \quad (4)$$

where C_0 and C_e (mg L^{-1}) are the concentration at initial and equilibrium, respectively. q_e (mg g^{-1}) is the adsorption capacity at equilibrium. M (g) is the amount of the adsorbent and V (L) is the volume of the solution.

2.7 Electro-Fenton process

The experiments were conducted in a batch reactor equipped with two graphite electrodes, which were situated 3 cm apart from each other. The current was supplied by a DC power supply. 0.1 L of aqueous synthetic wastewater was applied for the each experiment. The electrolyte was continuously stirred by the magnet. Prior to electro-Fenton reaction, O_2 was introduced into the solution for 5 min and then the electrical current between the two electrodes was applied to produce H_2O_2 at the cathode surface. At certain time intervals, 3 mL sample was collected from the solution and centrifuged. The visible light absorbance was at 358 nm. The removal efficiency was calculated by Eq. (5).

$$D(\%) = \frac{C_0 - C_t}{C_0} \times 100 \quad (5)$$

where D is removal efficiency. C_0 and C_t are the initial and sample concentration of TC, respectively.

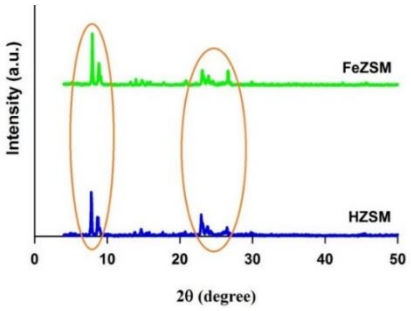

Fig. 2 XRD pattern of the nano-zeolites

Table 2 Crystallinity and textural data of the nano-zeolites

Sample	Crystallinity (%)	S_{BET} (m^2g^{-1})	V_{total} (cm^3g^{-1})	V_{micro} (cm^3g^{-1})	V_{meso} (cm^3g^{-1})
HZSM	100.00	321.10	0.19	0.13	0.06
FeZSM	98.19	318.80	0.20	0.12	0.08

3. Results and discussion

3.1 Characterization of nano-zeolite

The SEM images showed surface morphology of the parent and FeZSM nano-zeolites (Fig. 1). The FeZSM nano-zeolite had spherical morphology. It can be seen that there was no change in surface morphology after the impregnation of the parent nano-zeolite (Rostamizadeh *et al*. 2019). The XRD pattern of the samples confirmed the correct synthesis of ZSM-5 nano-zeolite (Fig. 2). The relative crystallinity was determined by peak area in region of 2θ = 22.5-25°, which was lower for the FeZSM nano-zeolite (Table 2) owing to pore blockage by iron species (Mohebbi *et al*. 2020). FT-IR spectra were recorded in the range of 400-4000 cm^{-1} (Fig. 3). The band around 550 cm^{-1} was related to the presence of five membered rings. The FT-IR bands in the range of 3500-3800 cm^{-1} are attributed to the surface hydroxyl groups. A broad band was seen around 3680 cm^{-1}, which was attributed to extra-framework

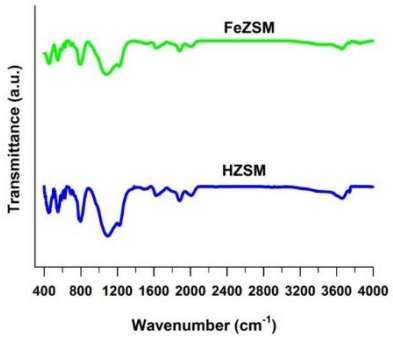

Fig. 3 FT-IR pattern of the nano-zeolites

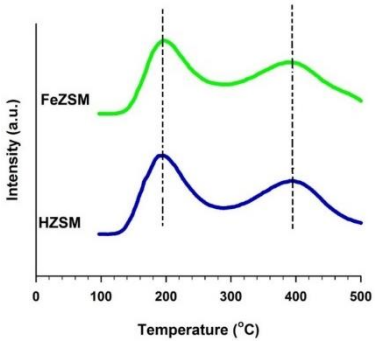

Fig. 5 Acidity of the nano-zeolites

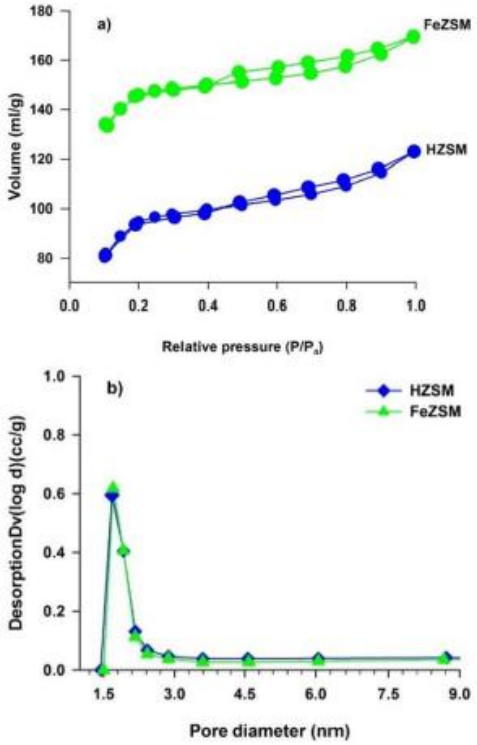

Fig. 4 (a) N_2 adsorption-desorption and (b) pore size distribution of the nano-zeolites

Table 3 Acidity data of the nano-zeolites

Sample	Acidity (mmol NH_3 g^{-1})			Strong/ Weak
	Weak	Strong	Total	
HZSM	0.53	0.53	1.06	1.00
FeZSM	0.44	0.53	0.97	1.20

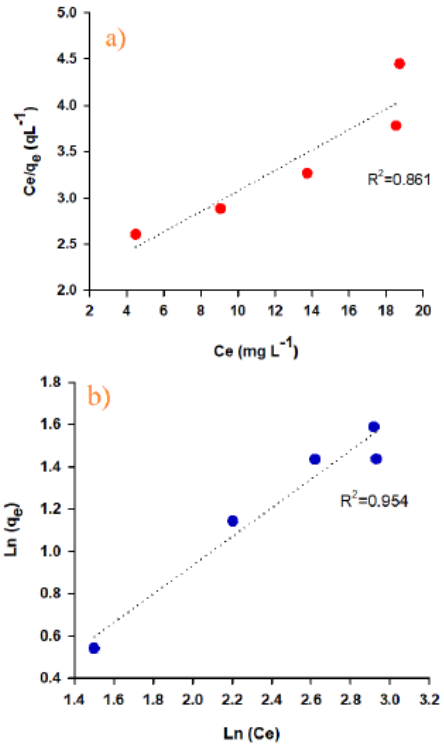

Fig. 6 Isotherm of TC removal (a) Langmuir and (b) Freundlich

aluminum species (Al-OH) in the nano-zeolite. The band at 3610 cm^{-1} and 3680 cm^{-1} were attributed to bridging Si-OH-Al (Rostamizadeh *et al*. 2018a). N_2 adsorption-desorption of nano-zeolite was a combination of isotherm types of I and IV (Fig. 4(a)). Adsorption at the low relative pressures ($\frac{P}{P_0} = 0.1$) indicated the formation of micro porous in the structure (Kianfar *et al*. 2018, Mahboub *et al*. 2016). The pore size distribution of FeZSM nano-zeolite reflected the formation of mesoporous structure (Fig. 4(b)). The FeZSM nano-zeolite involved the major pore diameter of 1.70 nm. The BET surface area of HZSM and FeZSM samples were 321.10 and 318.80 m^2g^{-1}, respectively (Table 2). The reduction of the specific surface area can be attributed to the blockage of the pores by the iron species (Chen *et al*. 2010). The NH_3-TPD measurements showed the similar patterns for the HZSM and FeZSM nano-zeolites (Fig. 5). The patterns included two peaks at low temperature and high temperature, indicating the weak and strong acid sites, respectively. The density of weak acidity decreased from 0.53 to 0.44 after the impregnation (Table 3). This result can be attributed to the blockage or neutralization of the sites by iron species.

3.2 Adsorption isotherms

The adsorption isotherm plays a key role in the design

Table 4 Equilibrium adsorption data

Isotherm models	Temperature (°C)	Parameters isotherm
Langmuir		
q_{max} (mg g^{-1})	9.049	
K_L (L mg^{-1})	0.056	25
R^2	0.861	
Freundlich		
K_f ((mg g^{-1}) (L $mg^{-1})^{1/n}$)	0.655	
1/n	0.678	25
R^2	0.954	

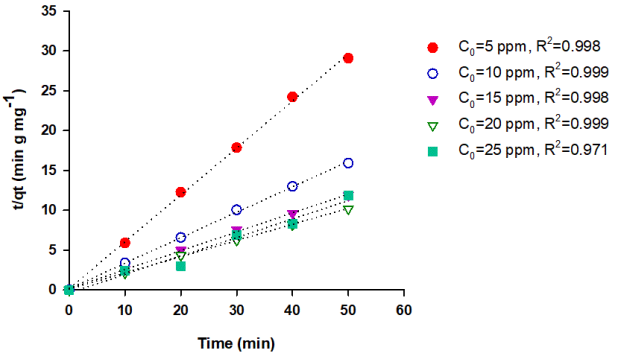

Fig. 7 Pseudo-second-order kinetic of TC adsorption. Conditions: V = 100 mL and 0.3 gL^{-1} FeZSM

Table 5 Kinetic data of TC adsorption over FeZSM

C_0 (mg L^{-1})	$q_{e,exp}$ (mg g^{-1})	Pseudo-second-order	
		$q_{e,cal}$ (mg g^{-1}) K_2 (g mg^{-1} min^{-1}) R^2	K_2 (g mg^{-1} min^{-1})
5 1.699	2.053	0.998	1.720
10 3.126	0.646	0.999	3.140
15 4.215	0.319	0.998	4.208
20 4.928	0.395	0.999	4.900
25 4.323	0.146	0.971	4.213

of adsorption systems. In this study, two important isotherms were investigated for the adsorption of TC on FeZSM nano-zeolite. The Langmuir isotherm is based on adsorption on uniform surfaces with equal energy that occurs as a monolayer on the adsorbent. The linear equation is as follows (Langmuir 1918).

$$\frac{C_e}{q_e} = \frac{1}{k_L q_{max}} + \frac{C_e}{q_{max}} \quad (6)$$

where q_e (mg g^{-1}) is equilibrium adsorption capacity and q_{max} (mg g^{-1}) indicates monolayer adsorption capacity. C_e is

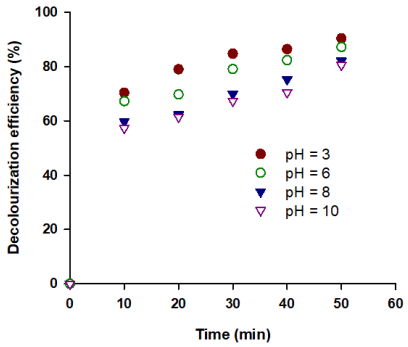

Fig. 8 TC removal efficiency at different solution pH levels. Reaction conditions: [Na_2SO_4] = 0.05 M, V = 100 mL, 0.3 gL^{-1} FeZSM, C_0 = 10 mg L^{-1}, I = 150 mA

the equilibrium concentration of TC and k_L (mg g^{-1}) is the constant Langmuir equilibrium. The Freundlich isotherm is based on the assumption of multi-layer sorption. The linear equation is as follows (Freundlich and Hatfield 1926).

$$\ln q_e = \ln k_f + \frac{1}{n} \ln c_e \quad (7)$$

where k_f and n are Freundlich isotherm constants. The Langmuir and Freundlich isotherms are shown in Fig. 6. The parameters of the models are summarized in Table 4. The Freundlich isotherm represented the experimental data very well. The obtained correlation coefficient for the Freundlich model was 0.954. Furthermore, the adsorption is desirable if $0 < \frac{1}{n} < 1$. Therefore, $\frac{1}{n} = 0.678$ showed that adsorption of TC over FeZSM was desirable.

3.3 Adsorption kinetics

The kinetic of TC adsorption was studied using pseudo-second-order models. TC adsorption kinetic on FeZSM nano-zeolite was well described by pseudo-second-order model. The linear equation can be expressed as following

$$\frac{t}{q_t} = \frac{1}{k_2 q_e^2} + \frac{1}{q_e} t \quad (8)$$

where q_e and q_t (mg g^{-1}) are the TC adsorption capacity at equilibrium and at different time t (min), respectively. k_2 (g mg^{-1} min^{-1}) is the rate constant of adsorption. The pseudo-second-order model with the high correlation coefficient (R^2 = 0.99) were the inconsistent with TC adsorption on FeZSM nano-zeolite (Fig. 7). The obtained results for the kinetic model are presented in Table 5. The calculated value of q_e were in well agreement with the experimental q_e, which confirmed pseudo-second-order kinetic for TC adsorption over the FeZSM nano-zeolite.

3.4 Electro-Fenton process

3.4.1 Effect of solution pH

pH is one of the important parameters in the electro-Fenton process. Fig. 8 shows the performance of FeZSM as

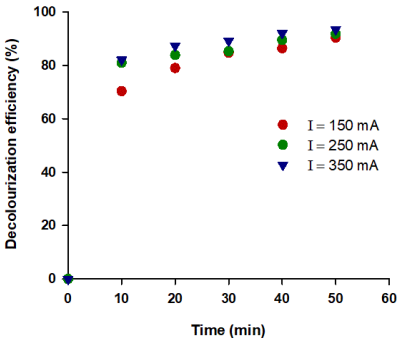

Fig. 9 TC removal efficiency at different current density. Reaction conditions: [Na_2SO_4] = 0.05 M, pH = 3, V = 100 mL, 0.3 gL^{-1} FeZSM, C_0 = 10 mg L^{-1}

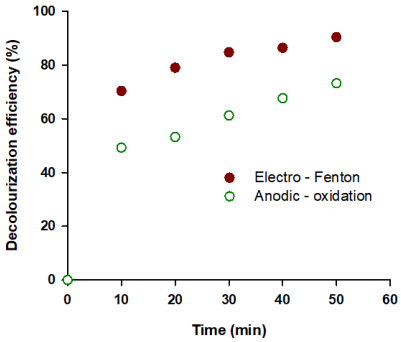

Fig. 10 Effect of FeZSM in TC removal efficiency through electro-Fenton process. Reaction conditions: [Na_2SO_4] = 0.05 M, V = 100 mL, 0.3 gL^{-1} FeZSM for electro-Fenton process, C_0 = 10 mg L^{-1}, I = 150 mA

catalyst at different pH values in the range of 3-10. At pH = 3, the highest removal efficiency of TC was obtained (90.35%). This agrees with the reported optimal value for the Fenton's reagent (Rostamizadeh *et al.* 2019). By increasing of pH, H_2O_2 is converted to H_3O^+ by taking proton (H^+) (Eq. (9)), which is more stable than H_2O_2 (El-Ghenymy *et al.* 2012).

$$H_2O_2 + H^+ \rightarrow H_3O_2^+ \quad (9)$$

Increasing of pH from 3.0 to 6.0 led to a reduction in the efficiency of the TC removal. Alkaline pH resulted in the low rate of removal and the lower catalyst activity. This phenomenon can be explained by the formation of $Fe(OH)_2$ and $Fe(OH)_3$ by reaction with hydroxyl ions (OH^-). Low oxidation ability of $^{\cdot}OH$ at the higher pH levels (El-Desoky *et al.* 2010) and the unstable H_2O_2 in neutral pH, which decomposed to water and oxygen (Eq. (10)), decreased the removal (Marselli *et al.* 2003).

$$H_2O_2 \rightarrow H_2O + O_2 \quad (10)$$

TC has several polar/ionizable groups, including amino, carboxyl, phenol, alcohol, and ketone. It has three acid dissociation constants (pKa = 3.3, 7.7 and 9.7). TC is as cations when pH < 3.3, as zwitterions at 3.3 < pH < 7.7, and

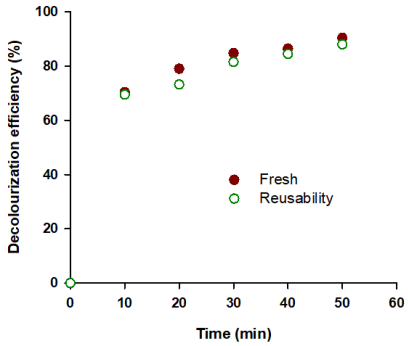

Fig. 11 Reusability of FeZSM catalyst for TC removal. Reaction conditions: [Na_2SO_4] = 0.05 M, V = 100 mL, 0.3 gL^{-1} FeZSM, C_0 = 10 mg L^{-1}, I = 150 mA

as anions when pH > 7.7 (Gao *et al.* 2012). On the other hand, the pH_{pzc} for the FeZSM nano-zeolite is 3.9. Therefore, the catalyst surface in the pH_{pzc} < pH is negatively charged. In this case, an electrostatic repulsion occurred between the catalyst surface and the adsorbent at alkaline pH, leading to low adsorption of TC at the catalyst surface.

3.4.2 Effect of current density

The current density is an important factor in the electro-Fenton process. The TC removal of the electro-Fenton process at different current densities is shown in Fig. 9. With increasing of current density from 150 to 350 mA, a slight increase in removal efficiency was observed. This increase in removal percentage can be attributed to an increase in anodic oxidation with increasing current density (Liu *et al.* 2018). When the current density increased, the transformed O_2 to the solution was adsorbed into the cathode surface and then, in acidic conditions was reduced by H_2O_2 to electro chemical (Eq. (11)).

$$O_2 + 4H^+ + 4e^- \rightarrow 2H_2O \quad (11)$$

In addition, the increase in current density led to the regeneration of Fe^{2+} from Fe^{3+} (Eq. (12)) at the cathode surface (Özcan *et al.* 2016).

$$Fe^{3+} + e \rightarrow Fe^{2+} \quad (12)$$

In accordance with Faraday's law, further increase in current density caused more corrosion of the anode electrode surface (Akyol *et al.* 2013).

3.4.3 Anodic oxidation of TC

Anodic oxidation is one of the AOPs (Tröster *et al.* 2002). In this process, $^{\cdot}OH$ is generated electrochemically in an anodic reaction directly from water (Eq. (13)) (Kraft *et al.* 2003, Marselli *et al.* 2003).

$$H_2O \rightarrow {}^{\cdot}OH + e^- + H^+ \quad (13)$$

We carried out a run with using no amount of catalyst (anodic oxidation). The results indicated a low removal

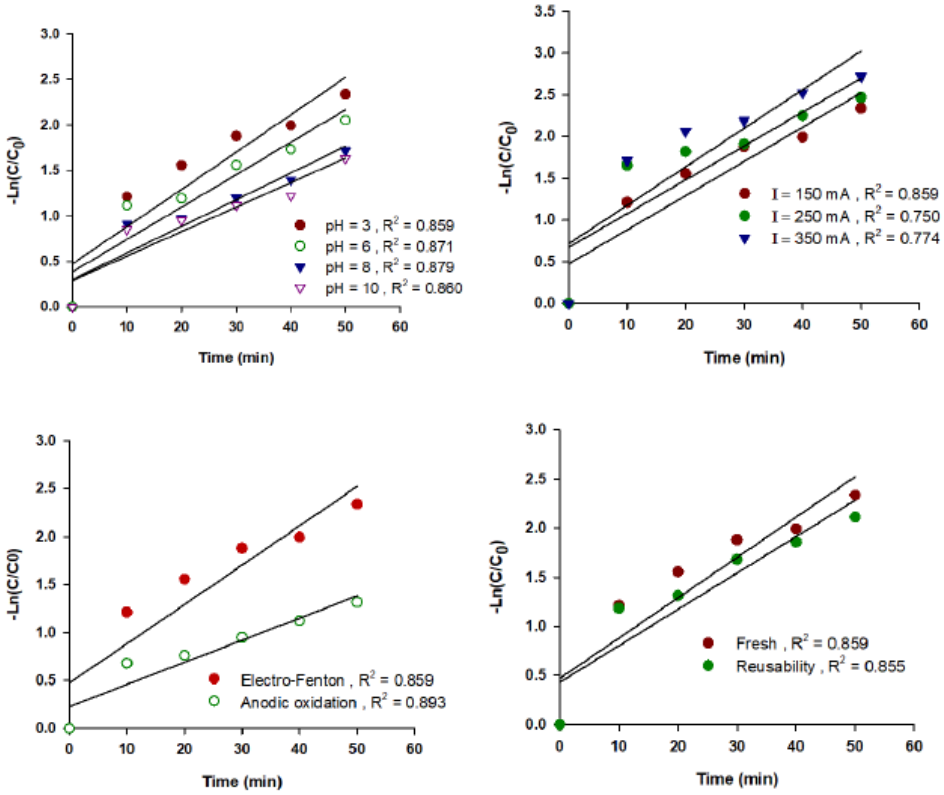

Fig. 12 Kinetic of TC removal at different operation conditions. Fixed reaction condition: [Na_2SO_4] = 0.05 M, V = 100 mL, C_0 = 10 mg L^{-1}, I = 150 mA

efficiency of TC (ca. 73.15%) through at 50 min (Fig. 10). However, addition of 0.3 gL^{-1} FeZSM catalyst increased the removal efficiency from 73.15% to 90.35%. This result confirmed the high performance of the FeZSM nano-zeolite in TC removal through electro-Fenton process.

3.5 Catalyst reusability

FeZSM catalyst including 0.5 wt% Fe was applied for the TC removal in sequence cycles. After the first run, the used catalyst was recovered by centrifugation. The regeneration of catalyst was at 550°C for 6 h (3°C min^{-1}) to remove organic species adsorbed on active sites. Fig. 11 shows the performance of the fresh and regenerated catalysts. A low reduction of the removal efficiency can be attributed to the poisoning of active sites and the oxidation of iron Fe^{2+} to Fe^{3+}. The regenerated FeZSM resulted in the high removal efficiency (ca. 87.92%). This phenomenon can be justified by the high surface area and total pore volume of nano-zeolite. The results confirmed the high stability of the catalyst in sequence cycles.

3.6 Eelctro-Fenton process kinetic

In this study, kinetic of TC removal in the electro-Fenton process was studied using pseudo-first-order model. The equation is

$$\ln(\frac{C}{C_0}) = -kt \qquad (15)$$

where C and C_0 (ppm) are the residual and initial TC concentrations, respectively. K (min^{-1}) is rate constant of pseudo-first-order kinetic and t (min) represents time. Fig. 12 shows kinetic of TC removal at different operating conditions. For all conditions, the pseudo-first-order kinetic model with significant amount of correlation coefficients showed the good agreement with the experimental data of TC removal in the electro-Fenton process.

4. Conclusions

In this study, the adsorption and electro-Fenton performance of FeZSM nano-zeolite including 0.5 wt% Fe were studied for TC removal. The parent HZSM-5 nano-zeolite was prepared by hydrothermal method and iron promoter was introduced through impregnation process. Langmuir and Freundlich isotherm models were determined to describe the adsorption mechanism of TC over FeZSM nano-zeolite. The experimental results showed the well agreement with the Freundlich isotherm. The adsorption of TC was modeled by pseudo-second-order kinetic model (R^2 = 0.999). In electro-Fenton process, the operation conditions including pH level of 3.0, 150 mA, 10 mg L^{-1} of TC concentration, and catalyst amount of 0.3 gL^{-1} resulted in the highest removal efficiency (ca. 90.35%). The developed nano-zeolite showed the appropriate reusability. The pseudo-first-order kinetic model was inconsistent with experimental data of TC removal in the electro-Fenton process.

Competing interests

The authors declare that they have no competing interest.

Ethical issues

Hereby, it is declared that this work and obtained results are original experimental work of authors and it has neither been published, nor is it under review in another journal, and it is not being submitted for publication in any other journals.

Authors' contributions

This work is the result of full co-operation of all mentioned authors.

References

Akyol, A., Can, O.T., Demirbas, E. and Kobya, M. (2013), "A comparative study of electrocoagulation and electro-Fenton for treatment of wastewater from liquid organic fertilizer plant", *Sep. Purif. Technol.*, **112**, 11-19. https://doi.org/10.1016/j.seppur.2013.03.036.

Ali, I., Singh, P., Aboul-Enein, H.Y. and Sharma, B. (2009), "Chiral analysis of ibuprofen residues in water and sediment", *Anal. Lett.*, **42**, 1747-1760. https://doi.org/10.1080/00032710903060768.

Álvarez-Torrellas, S., Rodríguez, A., Ovejero, G. and García, J. (2016), "Comparative adsorption performance of ibuprofen and tetracycline from aqueous solution by carbonaceous materials", *Chem. Eng. J.*, **283**, 936-947. https://doi.org/10.1016/j.cej.2015.08.023.

Basu, S. and Barman, S. (2019), "Adsorptive removal of fipronil from its aqueous solution by modified zeolite HZSM-5: Equilibrium, kinetic and thermodynamic study", *J. Mol. Liq.*, **283**, 867-878. https://doi.org/10.1016/j.molliq.2019.02.140.

Brillas, E., Sirés, I. and Oturan, M.A. (2009), "Electro-Fenton process and related electrochemical technologies based on Fenton's reaction chemistry", *Chem. Rev.*, **109**, 6570-6631. https://doi.org/10.1021/cr900136g.

Chen, L., Zhu, S.Y., Wang, Y.M. and He, M.Y. (2010), "One-step synthesis of hierarchical pentasil zeolite microspheres using diamine with linear carbon chain as single template", *New J. Chem.*, **34**, 2328-2334. https://doi.org/10.1039/C0NJ00316F.

Chopra, I. and Roberts, M. (2001), "Tetracycline antibiotics: mode of action, applications, molecular biology, and epidemiology of bacterial resistance", *Microbiol. Mol. Biol. Rev.*, **65**, 232-260. https://doi.org/10.1128/MMBR.65.2.232-260.2001.

Chu, W., Li, X., Zhu, X., Xie, S., Guo, C., Liu, S., Chen, F. and Xu, L. (2017), "Size-controlled synthesis of hierarchical ferrierite zeolite and its catalytic application in 1-butene skeletal isomerization", *Microporous Mesoporous Mater.*, **240**, 189-196. https://doi.org/10.1016/j.micromeso.2016.11.015.

El-Desoky, H.S., Ghoneim, M.M., El-Sheikh, R. and Zidan, N.M. (2010), "Oxidation of Levafix CA reactive azo-dyes in industrial wastewater of textile dyeing by electro-generated Fenton's reagent", *J. Hazard. Mater.*, **175**, 858-865. https://doi.org/10.1016/j.jhazmat.2009.10.089.

El-Ghenymy, A., Garcia-Segura, S., Rodríguez, R.M., Brillas, E., El Begrani, M.S. and Abdelouahid, B.A. (2012), "Optimization of the electro-Fenton and solar photoelectro-Fenton treatments of sulfanilic acid solutions using a pre-pilot flow plant by response surface methodology", *J. Hazard. Mater.*, **221**, 288-297. http://dx.doi.org/10.1016/j.jhazmat.2012.04.053.

Eliopoulos, G.M., Eliopoulos, G.M. and Roberts, M.C. (2003), "Tetracycline therapy: update", *Clin. Infect. Dis.*, **36**, 462-467. https://doi.org/10.1086/367622.

Freundlich, H. and Hatfield, H.S. (1926), *Colloid and Capillary Chemistry*, Methuen And Co. Ltd., London, UK. https://doi.org/10.1021/ed003p1454.2.

Gao, Y., Li, Y., Zhang, L., Huang, H., Hu, J., Shah, S.M. and Su, X. (2012), "Adsorption and removal of tetracycline antibiotics from aqueous solution by graphene oxide", *J. Colloid Interface Sci.*, **368**, 540-546. https://doi.org/10.1016/j.jcis.2011.11.015.

Ghadim, E.E., Manouchehri, F., Soleimani, G., Hosseini, H., Kimiagar, S. and Nafisi, S. (2013), "Adsorption properties of tetracycline onto graphene oxide: Equilibrium, kinetic and thermodynamic studies", *PLoS One*, **8**, e79254. https://doi.org/10.1371/journal.pone.0079254.

Gharibian, S., Hazrati, H. and Rostamizadeh, M. (2020), "Continuous electrooxidation of methylene blue in filter press electrochemical flowcell: CFD simulation and RTD validation", *Chem. Eng. Process*, **150**, 107880. https://doi.org/10.1016/j.cep.2020.107880.

Huang, L., Wang, M., Shi, C., Huang, J. and Zhang, B. (2014), "Adsorption of tetracycline and ciprofloxacin on activated carbon prepared from lignin with H3PO4 activation", *Desalin. Water Treat.*, **52**, 2678-2687. https://doi.org/10.1080/19443994.2013.833873.

Ifebajo, A.O., Oladipo, A.A. and Gazi, M. (2019), "Efficient removal of tetracycline by CoO/$CuFe_2O4$ derived from layered double hydroxides", *Environ. Chem. Lett.*, **17**, 487-494. https://doi.org/10.1007/s10311-018-0781-0.

Kianfar, E., Salimi, M., Pirouzfar, V. and Koohestani, B. (2018), "Synthesis of modified catalyst and stabilization of CuO/NH4-ZSM-5 for conversion of methanol to gasoline", *Int. J. Appl. Ceram. Technol.*, **15**, 734-741. https://doi.org/10.1111/ijac.12830.

Kraft, A., Stadelmann, M. and Blaschke, M. (2003), "Anodic oxidation with doped diamond electrodes: A new advanced oxidation process", *J. Hazard. Mater.*, **103**, 247-261. https://doi.org/10.1016/j.jhazmat.2003.07.006.

Langmuir, I. (1918), "The adsorption of gases on plane surfaces of glass, mica and platinum", *J. Am. Chem. Soc.*, **40**, 1361-1403. https://doi.org/10.1021/ja02242a004

Liu, D., Zhang, H., Wei, Y., Liu, B., Lin, Y., Li, G. and Zhang, F. (2018), "Enhanced degradation of ibuprofen by heterogeneous electro-Fenton at circumneutral pH", *Chemosphere*, **209**, 998-1006. https://doi.org/10.1016/j.chemosphere.2018.06.164.

Mahboub, M.J.D., Rostamizadeh, M., Dubois, J.I. and Patience, G.S. (2016), "Partial oxidation of 2-methyl-1, 3-propanediol to methacrylic acid: Experimental and neural network modeling", *RSC Adv.*, **6**, 114123-114134. https://doi.org/10.1039/C6RA16605A.

Marselli, B., Garcia-Gomez, J., Michaud, P.A., Rodrigo, M. and Comninellis, C. (2003), "Electrogeneration of hydroxyl radicals on boron-doped diamond electrodes", *J. Electrochem. Soc.*, **150**, 79-83. https://doi.org/10.1149/1.1553790.

Martínez-Huitle, C.A. and Brillas, E. (2008), "Electrochemical alternatives for drinking water disinfection", *Angew. Chem. Int. Ed.*, **47**, 1998-2005. https://doi.org/10.1002/anie.200703621.

Mohebbi, S., Rostamizadeh, M. and Kahforoushan, D. (2020), "Effect of molybdenum promoter on performance of high silica MoO3/B-ZSM-5 nanocatalyst in biodiesel production", *Fuel*, **266**, 117063. https://doi.org/10.1016/j.fuel.2020.117063.

Özcan, A., Özcan, A.A. and Demirci, Y. (2016), "Evaluation of mineralization kinetics and pathway of norfloxacin removal from water by electro-Fenton treatment", *Chem. Eng. J.*, **304**,

518-526. https://doi.org/10.1016/j.cej.2016.06.105.
Panizza, M. and Cerisola, G. (2009), "Direct and mediated anodic oxidation of organic pollutants", *Chem. Rev.*, **109**, 6541-6569. https://doi.org/10.1007/978-1-4419-6996-5_126.
Puga, A., Rosales, E., Pazos, M. and Sanromán, M. (2020), "Prompt removal of antibiotic by adsorption/electro-Fenton degradation using an iron-doped perlite as heterogeneous catalyst", *Process Saf. Environ. Prot.*, **144**, 100-110. https://doi.org/10.1016/j.psep.2020.07.021.
Rostamizadeh, M. and Rizi, S.M.H. (2012), "Predicting gas flux in silicalite-1 zeolite membrane using artificial neural networks", *J. Membr. Sci.*, **403**, 146-151. http://dx.doi.org/10.1016/j.memsci.2012.02.036.
Rostamizadeh, M., Yaripour, F. and Hazrati, H. (2018a), "High efficient mesoporous HZSM-5 nanocatalyst development through desilication with mixed alkaline solution for methanol to olefin reaction", *J. Porous Mater.*, **25**, 1287-1299. https://doi.org/10.1007/s10934-017-0539-2.
Rostamizadeh, M., Yaripour, F. and Hazrati, H. (2018b), "Selective production of light olefins from methanol over desilicated highly siliceous ZSM-5 nanocatalysts", *Polyolefins J.*, **5**, 59-70. https://doi.org/10.22063/poj.2017.1501.
Rostamizadeh, M., Jalali, H., Naeimzadeh, F. and Gharibian, S. (2019), "Efficient removal of diclofenac from pharmaceutical wastewater using impregnated zeolite catalyst in heterogeneous Fenton process", *Phys. Chem. Res.*, **7**, 37-52. https://doi.org/10.22036/pcr.2018.144779.1524.
Tröster, I., Fryda, M., Herrmann, D., Schäfer, L., Hänni, W., Perret, A., Blaschke, M., Kraft, A. and Stadelmann, M. (2002), "Electrochemical advanced oxidation process for water treatment using DiaChem® electrodes", *Diamond Relat. Mater.*, **11**, 640-645. https://doi.org/10.2166/wst.2004.0264.
Vosoughi, M., Fatehifar, E., Derafshi, S. and Rostamizadeh, M. (2017), "High efficient treatment of the petrochemical phenolic effluent using spent catalyst: Experimental and optimization", *J. Environ. Chem. Eng.*, **5**, 2024-2031. https://doi.org/10.1016/j.jece.2017.04.003.
Xue, Z., Wang, T., Chen, B., Malkoske, T., Yu, S. and Tang, Y. (2015), "Degradation of tetracycline with BiFeO3 prepared by a simple hydrothermal method", *Materials*, **8**, 6360-6378. https://doi.org/10.3390/ma8095310.
Yahya, M.S., Oturan, N., El Kacemi, K., El Karbane, M., Aravindakumar, C. and Oturan, M.A. (2014), "Oxidative degradation study on antimicrobial agent ciprofloxacin by electro-Fenton process: Kinetics and oxidation products", *Chemosphere*, **117**, 447-454. https://doi.org/10.1016/j.chemosphere.2014.08.016.

CC